Acta Polytechnica **63**(3):158–170, 2023
https://doi.org/10.14311/AP.2023.63.0158

Published by the Czech Technical University in Prague

FRACTIONAL MULTI-LOOP ACTIVE DISTURBANCE REJECTION CONTROL FOR A LOWER KNEE EXOSKELETON SYSTEM

Nasir Ahmed Al-Awad[a,*], Amjad Jaleel Humaidi[b], Ahmed Sabah Al-Araji[c]

[a] *University of Mustansiriyah, Department of Computer Engineering, 10001 Baghdad, Iraq*

[b] *University of Technology, Control and Systems Engineering Department, 10066 Baghdad, Iraq*

[c] *University of Technology, Department of Computer Engineering, 10066 Baghdad, Iraq*

[*] corresponding author: cse.20.33@grad.uotechnology.edu.iq

Abstract. Rehabilitation Exoskeleton is becoming more and more important in physiotherapists' routine work. To improve the treatment performance, such as reducing the recovery period and/or monitoring and reacting to unpredictable situations, the rehabilitation manipulators need to help the patients in various physical trainings. A special case of the active disturbance rejection control (ADRC) is applied to govern a proper realisation of basic limb rehabilitation trainings. The experimental study is performed on a model of a flexible joint manipulator, whose behaviour resembles a real exoskeleton rehabilitation device (a one-degree-of-freedom, rigid-link, flexible-joint manipulator). The fractional (FADRC) is an unconventional model-independent approach, acknowledged as an effective controller in the existence of total plant uncertainties, and these uncertainties are inclusive of the total disturbances and unknown dynamics of the plant. In this work, three FADRC schemes are used, the first one using a fractional state observer (FSO), or FADRC1, second one using a fractional proportional-derivative controller (FPD), or FADRC2, and the third one a Multi-loop fractional in PD-loop controller and the observer-loop (Feedforward and Feedback), or FADRC3. The simulated Exoskeleton system is subjected to a noise disturbance and the FADRC3 shows the effectiveness to compensate all these effects and satisfies the desired position when compared with FADRC1 and FADRC2. The design and simulation were carried out in MATLAB/Simulink.

Keywords: ADRC, fractional calculus, exoskeleton system, exogenous disturbance, extended state observer.

1. Introduction

An exoskeleton is an electromechanical framework that reflects the form and function of the body of an operator wearing it. In rehabilitation, robotics is a new topic that is believed to be a promising way to automate training. Robotic rehabilitation can take the place of a therapist's physical training activities, allowing for more rigorous repeated motions and lower therapy costs [1]. Fixed trajectory controllers move the user's limb along a predefined movement path. They provide the smallest amount of freedom because user engagement is not taken into account [2]. There has been a substantial amount of research in several sectors required for developing and increasing the performance of these devices, and there are numerous obstacles in this area, one of the most important of them being the system control. The exoskeleton control scheme can be divided into position, torque/force, and force interaction controllers based on physical factors. To ensure that the exoskeleton joints revolve at the proper angle, the position control technique is typically used. Some exoskeleton axes have fixed joint positions due to rehabilitation goals. The PD position controller is used for these axes, and the axes are locked at a specified angle position [3–5].

Exoskeletons with many degrees of freedom have been implemented with proportional-integral-derivative (PID) controllers to control the leg's motion, despite its ease of implementation, the usage of PID control is limited by the convergence analysis and coefficient adjustments [6]. A backstepping controller based on the shank-orthosis system was proposed, where backstepping can commonly address stability, monitoring, and robustness control problems under less restrictive settings than other methods [7, 8].

In recent years, a fuzzy controller with a bang-bang controller with a high accuracy and fast response has been proposed for the output torque control. An adaptive self-organising fuzzy controller is developed for the rehabilitation Exoskeleton in this study, its fuzzy sliding surface can help to reduce the number of fuzzy rule [9]. The self-organising learning mechanism is employed to modify fuzzy rules in real time. A collection of fuzzy IF-THEN rules is used to create an intelligent lower extremity rehabilitation training system controlled by fuzzy or adaptive fuzzy controllers [10, 11]. As a result, another intelligent control system based on a neuro-fuzzy controller for upper limbs was suggested in [12], to construct a power assist exoskeleton. In order to achieve an accurate control performance,

ANN-based model predictive control (MPC) methods are used, despite the ability to approximate nonlinear properties, real-time performance is constrained, and all of these control applications are limited [13].

Any system uncertainties, such as exogenous disruptions, unmodelled dynamics, and parameter perturbations, have a significant impact on the performance of a control system. The development of the any controller that attempts to fulfil these objectives while also assuring disturbance rejection and strong tracking performance in the face of huge uncertainty is complicated [14]. Because of this, anti-disturbance approaches are used for both external and internal loop controllers and estimators have been widely employed [15].

Regarding the biomechanics of the exoskeleton, a sliding mode control (SMC) may be an appropriate solution due to its robustness to both internal and external system uncertainties. One of these solutions proposed a control scheme with a model-free decentralised output feedback adaptive high-order sliding mode control to solve the trajectory tracking problem in each degree of freedom of the exoskeleton. In this work, a second-order adaptive sliding mode controller based on the super-twisting algorithm drives the exoskeleton articulations to track the proposed reference trajectories [16]. The main problem of the SMC is the chattering. Many studies partly solved this thanks to the ability of the Exoskeleton to follow the optimised trajectories [17]. To achieve an optimal performance, the SMC parameters should be chosen carefully. Genetic Algorithm GA [18], Particle Swarm Optimization PSO [19], Grey-wolf optimization [20], and Ant colony optimization [21] are examples of common optimisation methods that are used in exoskeleton devices. GA is used to determine the optimal sliding surface and the sliding control law. It is easy to use and capable of finding global optima, which can be used to improve the structure of optimisation systems [22].

Many works also deal with the reduction of chattering by employing a synergetic control (SC) technique. This control methodology has been used to govern highly coupled and complicated nonlinear systems. The SC is based on state-space theory. An independent manifold is developed to fulfil the necessary control criteria in the situation of parametric and nominal uncertainty, and a controller constructed based on SC might drive the system's state variables in such a manner as to track it. It eliminates chattering while maintaining the same control systems as SMC [23].

The ADRC is a modern robustness regulation conceptual model based on the standard PID control algorithm, first introduced in [24], and further developed in [25]. The ADRC has recently been used in the field of rehabilitation systems [26, 27]. The ADRC was created by merging ESO with a variety of control approaches.

Fractional order controllers, like CRONE control and expanded fractional control theories based on adaptive control and sliding mode control, have produced improved results in both theory and practice [28, 29]. The fractional order control has been investigated in robotic and engineering systems and used to obtain reliable performances in industrial systems, despite its inherent complexity [30–33]. Later, utilising various tuning techniques and numerical optimisation, several researchers focused on the design and synthesis of FOPID controllers [34].

The classical extended states observer (ESO) is generalised to a fractional order extended states observer (FESO) in FADRC [35], using fractional calculus. Numerous studies show that the fraction-order active disturbance rejection controller (FADRC) outperforms the integer-order ADRC in terms of robustness, disturbance rejection, and parameter variation uncertainty capacity [36–38].

In terms of robustness against noisy environments and perturbation, some researchers have suggested a FADRC control system that consists of a proportional controller and a fraction-order ESO [39]. In contrast, other researchers have suggested an ADRC and fraction-order PID (FOPID) direct torque control technique for the hydro-turbine speed governor system that is load-disturbance tolerant, since the integer order ESO (IESO) has weak high-frequency disturbance prediction capabilities [40]. In order to improve the performance of the system's control, a FADRC typically offered a control technique based on a fraction-order ESO (FESO) [35]. The paper's contribution can be highlighted by the following points:

I. In order to increase the lower limb exoskeleton system's ability to reject disturbances and achieve limited convergence, FADRC has been introduced in this research.

II. There is evidence for the controlled system's robustness and better convergence properties to satisfy the stability.

III. A comparison study have been conducted between the proposed FADRC3 and two configurations of FADRC, focusing on error performance indices and the control torque required with minimal chattering.

The paper is organised into several sections. Section 2 introduces the structure, mathematical model calculations of the proposed exoskeleton, and ADRC methodology. Stability analysis is presented in Section 3. Section 4 shows the simulation results and discussion about the system. Conclusions and future work are discussed in Section 5.

2. Materials and Methods

The fundamental ideas underlying the knee-joint mathematical model, the ADRC control components, and the proposed controllers are established in this part.

2.1. Modelling of Lower Limb Robotic Rehabilitation Exoskeleton

The active exoskeleton electromechanical device described in this study is worn by a human operator and is intended to improve the wearer's physical performance. Direct motor driving through reducers provides the action of the hip and knee. The exoskeleton's swing leg is the primary focus of the effort. Generally, the dynamic model of the lower knee joint motion is [41–43]:

$$J\ddot{\theta} = -\tau_g cos\theta - Asgn\dot{\theta} - B\dot{\theta} + \tau_c + \tau_h\,. \qquad (1)$$

The angular position θ is the knee joint angle between the actual position of the shank and the full extension position, $\dot{\theta}$ and $\ddot{\theta}$ are the knee joint angular velocity and acceleration, respectively. J, A, B, τ_g, τ_c, τ_h are the Inertia, solid friction coefficient, viscous friction coefficient, gravity torque, controller torque and human torque, respectively. Based on the mathematical equation above, designers can see that the system is inherently nonlinear due to nonlinear terms like cos and sign, which makes it difficult to evaluate; nevertheless, the ADRC Handle System has the advantage of being able to control system dynamics as a linear controller. The single control variable in this work is the position (θ), which must be regulated according to a specified trajectory. Subjects rested upright on a treatment table in a fixed state, with the shank hanging off the table at roughly -45 degrees, which is the rest position. The formal testing consisted of the following trials that were completed in a specific sequence. moving to an angle of -45 degrees of knee flexion to reach -90 degrees, and then returning to -45 degrees, after that, moving to an angle of 0 degrees of knee flexion and returning to -45 degrees (Initial condition). This training was repeated every 4 seconds. The flat series of Maxon's EC90 brushless DC motors was used for the exoskeleton. It can provide a constant torque of up to 560 mN·m. This motor was chosen because it is among the cheapest and smallest models on the market, making it suitable for use in the exoskeleton. Figure 1 shows the structure of the exoskeleton. The parameters of the exoskeleton system used in this study has been listed in Table 1 [41].

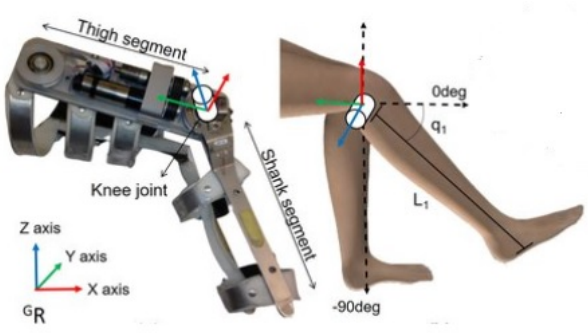

Figure 1. Lower Limb Robotic Rehabilitation Exoskeleton [41].

Parameter	Value
Inertia (J)	0.348 Kg·m^2
Solid Friction Coefficient (A)	0.998 N·m
Viscous Friction Coefficient (B)	0.872 N·m·s·rad^{-1}
Gravity Torque	3.445 N·m

Table 1. Parameters of the exoskeleton [41].

2.2. ADRC Methodology

The primary concept of ADRC is disturbance rejection, which is based on the lack of a precise mathematical model of the system [43, 44]. The ESO is utilised in the ADRC framework to estimate the disturbance so that it can later be terminated in the control rule. The ADRC is a form of nonlinear control approach that comes in two types.

2.2.1. Linear ADRC (LADRC)

The ADRC is mainly composed of tracking differential (TD), extended state observer (ESO), and state error feedback (SEF). A general nth-order SISO dynamical system, which may be used to describe a wide range of physical systems, can be formulated as a fundamental input-output representation for simplicity and without abandoning generality [25]:

$$y^{(n)} = f\left(y^{(n-1)}, y^{(n-2)}, \ldots, y\right) + W + b_0 u\,. \qquad (2)$$

According to Equation (1), one can have:

$$\ddot{\theta} = \ddot{y} = f(t, \theta, \dot{\theta}, W) + b_0 u\,, \qquad (3)$$

where u represents the control input (to be designed), (y) represents the only observable system output signal, W denotes the unidentified external disturbance, $f(.)$ demonstrates probably the most frequently unknown internal (state-dependent and feasibly nonlinear) dynamics of the process, and (b_0) signifies the unknown input correction factor.

The purpose of the control is to create a system input signal (u) that allows the system output (y) to track the target value (y_d), an irrespective influence of unmolded/unknown system components (seen as an acting perturbation). A new term (δ) can be introduced to tackle both the internal modelling mismatch $f(.)$ and the unknown external disturbance (W), resulting in a required generalised controllable canonical form of the system [15]:

$$\begin{aligned} y^{(n)} &= \delta + b_0 u\,, \\ \delta &= f(.) + W\,, \end{aligned} \qquad (4)$$

where (δ) is assumed to be the total disturbance. The modelling uncertainty related to (b) can also be treated as part of the total disturbance, so that Equation (4) can be written as:

$$\delta = f(.) + W + u(b - b_0)\,. \tag{5}$$

The plant model can be described using the state-space representation as:

$$\begin{aligned} \dot{x} &= Ax + Bu + E\delta\,, \\ y &= Cx\,. \end{aligned} \tag{6}$$

The plant matrices are placed in $(n+1)$ form because the ADRC needs an extra state for cancelling the total disturbances, then

$$x = [x_1, x_2, \ldots, x_n, x_{n+1}] \cong [y, \dot{y}, \ldots, y^n, \delta]\ . \tag{7}$$

The observer, in this case, takes the form of the most widely used linear Luenberger-like estimator, which is:

$$\begin{aligned} \dot{\hat{x}} &= A\hat{x} + Bu + L(x - \hat{x})\,, \\ y &= C\hat{x}\,. \end{aligned} \tag{8}$$

The aim is $(\hat{x} \to x)$, so that

$$\begin{aligned} \hat{x} &= [\hat{x}_1, \hat{x}_2, \ldots\ldots, \hat{x}_n, \hat{x}_{n+1}] \\ &\cong \left[\hat{y}, \hat{\dot{y}}, \ldots\ldots, \delta\right]\ , \end{aligned} \tag{9}$$

where, $L = [l_1, l_2, \ldots, l_n, l_{n+1}]$ represents the observer gains and depends on the observer's bandwidth (w_0). If one chooses $w_0 = 4w_c$, where w_c is the controller bandwidth, then it is easy to calculate the elements of the observer matrix gains $(l_1 = 3w_o, l_2 = 3w_o^2, l_3 = w_o^3)$ according to [25]. The second part of the ADRC is the state error feedback (SEF). In this work, done by linear proportional-derivative controller (PD)

$$u_0 = K_p\epsilon + K_d\dot{\epsilon} = K_p(r - \hat{x}_1) + K_d(\dot{r} - \hat{x}_2)\,, \tag{10}$$

where K_p is the proportional gain and K_d is the derivative gain. These values are calculated from the controller bandwidth (w_c) and damping ratio (ς). These values depend on the design specifications [45],

$$\begin{aligned} K_p &= w_c^2\,, \\ K_d &= 2\varsigma w_c\,. \end{aligned} \tag{11}$$

In the ADRC technique, the control rule is composed of a controller (u_0), which is in charge of completing the assigned task (i.e. $y \to y_d$), and a disturbance rejection estimation term $(\hat{\delta})$, as shown below:

$$u = \frac{u_0 - \hat{\delta}}{b_0}\,, \tag{12}$$

where $\hat{\delta} = \hat{x}_3$ is the estimated total disturbance (in the system under test) and (u_0) is the proposed control signal for the currently disturbance-free system, which is designed to match some predetermined closed-loop requirements. The suggested control rule can be introduced in the extended system in each control cycle if the estimating loop is well tuned (i.e. $\hat{\delta} = \delta$), and this gives, theoretically:

$$y_n = \delta + \frac{b_0(u_0 - \delta)}{b_0} = u_0\,. \tag{13}$$

This reduces the system to a basic cascade of integrators, making it easier to govern due to the system's fundamental adaptability to any perturbation.

2.2.2. Fractional ADRC (FADRC)

In this work, we use three approaches of FADRC, the first approach, FADRC1, depends on an ESO modified to a fractional order extended states observer FESO, the second approach, FARC2, depends on a Fractional PD controller, and finally, the third one is the proposed controller, FADRC3, combining FADRC1 and FADRC2.

FADRC1 approach

All the Equations (3)-(12) for LADRC, can be used only by FESO, instead of linear LESO, so that we deal with modified ADRC (FADRC1). The definition of fractional calculus proposed by Caputo is widely used in fractional order control [46, 47]. The fractional calculus is a generalisation of integration and differentiation to a non-integer order operator:

$$D^{\alpha} = \begin{cases} \dfrac{d^{\alpha}}{d_t^{\alpha}} & for \alpha \succ 0 \\ 1 & for \alpha = 0 \\ \displaystyle\int_a^t (dt)^{-\alpha} & for \alpha \prec 0 \end{cases}\ , \tag{14}$$

where a and t denote the limits of the operation and (α) denotes the fractional order, which lies between (0 to 1). The important key in FADRC is the ESO, so that we can use the fractional order for the derivative in all estimate states of observer $\hat{x} = [\hat{x}_1, \hat{x}_2, \ldots\ldots, \hat{x}_n, \hat{x}_{n+1}]$. Equation (8) can be written as:

$$\begin{cases} D^{\alpha 1}\hat{x}_1 = \hat{x}_2 + l_1(y - \hat{x}_1) \\ D^{\alpha 2}\hat{x}_2 = \hat{x}_3 + Bu + l_2(y - \hat{x}_1) \\ D^{\alpha 3}\hat{x}_3 = l_3(y - \hat{x}_1) \end{cases}\ , \tag{15}$$

where the observers gains $L = [l_1, l_2, l_3]$ are determined by rules in [45], or using any optimisation methods. Figure 2. shows the general structure of FADRC1 for the Exoskeleton control system. The nonlinear structure (fractional term) is used in ESO

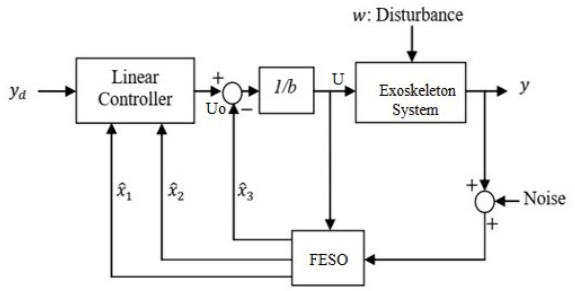

FIGURE 2. The general idea of FADRC1 for Exoskeleton control system.

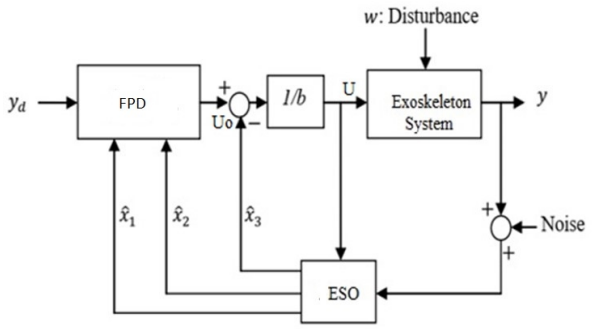

FIGURE 3. The general idea of FADRC2 for Exoskeleton control system.

to comprehensively estimate the un-modelled errors and external disturbances. In order for the FESO to estimate the state more quickly and accurately, and ultimately for the FADRC to achieve a superior control performance, the fractional-order integration has an additional weight function and the initial stage has a bigger integral response value. The FESO assesses both the overall disturbance and the variable structure dynamic states, resulting in a smaller observer bandwidth. Pursuing the analysis from [45], the bandwidth (w_c) is related to settling time (τ_s) of the closed-loop system, according to the following formula:

$$w_c = \frac{10}{\tau_s}\,. \tag{16}$$

In this application, the specification of the settling time of the controlled system is chosen to be τ_s = 0.408 s. The observer and PD controller gains can be calculated according to the above equation with (w_c = 24.5 rad·sec^{-1}). The best fractional observer terms ($\alpha_1, \alpha_2, \alpha_3$) values can be obtained by any optimisation algorithm [48–50]. In this work, PSO parameters are chosen according to the trial and error method as follows:

Iterations = 30; inertia = 1.5; c1 = 2; c2 =2; swarm_size = 30; no_of_param = 3;

The PSO optimisation result gives the best value of Fractional observer integrators terms ($\alpha_1, \alpha_2, \alpha_3$) as (0.5243, 1, 0.4513), respectively.

FADRC2 approach

In this section, we use the LADRC structure with only a PD controller modified by using fractional term of controller derivative:

$$u_0 = K_p \epsilon K_d D^{\alpha_\epsilon} \epsilon\,. \tag{17}$$

The controller parameters (K_p, K_d) are calculated according to Equation (11). One parameter to optimise for FADRC2 is the fractional term of derivative (α_c). The PSO optimisation result gives the best value of Fractional controller term (α_c) as (0.1419). Figure 3 shows the general structure of FADRC2 for the Exoskeleton control system.

FADRC3 approach

In this section, we combine the two approaches, FADRC1 for minimisation of the chattering and FADRC2 for reducing the error, to construct a multi-fractional approach FADRC3 for improving the trajectory performance and increase the response accuracy. The same design parameters for FADRC1 and FADRC2 are used in this proposed approach.

Integral of the absolute error (IAE), Integral square error (ISE), Integral square of the control signal (ISU), Integral absolute of the control signal (IAU), and root mean square error (R.M.S.E) are the performance indices chosen for evaluating and comparing the results. Each of these performance indices can be expressed as follows:

$$\begin{cases} IAE = \displaystyle\int_0^t |(y_d - y)|dt \\ ISE = \displaystyle\int_0^t (y_d - y)^2 dt \\ R.M.S.E = \sqrt{\dfrac{1}{n}\displaystyle\sum_1^n (y_d - y)^2}\,, \\ ISU = \displaystyle\int_0^t u^2 dt \\ IAU = \displaystyle\int_0^t |u| dt \end{cases} \tag{18}$$

where, (y_d) is the reference input signal, (y) is the output of the system, ($y_d - y$) denotes the error of the system, and (u) is the control output. The values were determined based on the minimum value of the index, which recommends the best performance [51, 52]. The IAU performance index provides a measure of chatter reduction in the control signal [53], whereas ISU refers to the controlling effort needed for a controller.

3. STABILITY ANALYSIS

One of the main issues in the control system design is how to guarantee the stability of the controlled

system [54]. In this part, the stability analysis will be conducted based on the pole-placement theory.

Lemma 1: Considering the system of Equation (3) with the parametric uncertainties f, the control law developed based on FADRC can lead to an asymptotic convergence of tracking error to zero for a given desired trajectory. This will give the condition of bounded-input bounded-output (BIBO) stability of the closed-loop system in terms of roots of a polynomial.

The stability analysis of the proposed control algorithm is initiated by letting:

$$\epsilon_i^{\alpha} = x_i^{\alpha} - \hat{x}^{\alpha}, \; i = 1, 2, 3, \dots , \tag{19}$$

where α is fractional term. Combining Equation (7) and Equation (15), the error equation is:

$$\epsilon_i^{\alpha} = A_{\epsilon}\epsilon_i + Eh\,. \tag{20}$$

Equation (20) can be represented as state-space:

$$A_{\epsilon} = \begin{bmatrix} -l_1 & 1 & 0 \\ -l_2 & 0 & 1 \\ -l_3 & 0 & 0 \end{bmatrix}, E = \begin{bmatrix} 0 \\ 0 \\ 1 \end{bmatrix}, h = f^{\alpha}(.)\,. \tag{21}$$

The characteristic polynomial of (A_{ϵ}) is [55]:

$$Q(s) = s^{3\alpha} + l_1 s^{2\alpha} + l_2 s^{\alpha} + l_3 = (s^{\alpha} + w_0)^3\,. \tag{22}$$

There are two boundary lines for the stable region with the slope $(\pm 0.5\pi\alpha)$. The stable region includes left half-plane, including the imaginary axis because of $(0 < \alpha < 1)$.

Transforming the above fractional-order system to w-plane by replacing $(s^{\alpha} = w)$, the transfer function is given by $Q(s) = (w + w_o)^3$. All the poles are determined at $(-w_o)$, i.e. at left half-plane. When the observer gain is selected sufficiently large, the FESO is BIBO stable and the whole closed-loop system is BIBO.

4. Results and Discussion

To verify the controller's robustness, FADRC will be simulated for two different cases in this part. The simulation results will be compared using many disturbances and noise criteria. The desired trajectory for training is a sinusoidal input with the starting angle of the exoskeleton of (-45 deg, or -0.785 rad), and the maximum angle of (-90 deg, or -1.57 rad), at knee flexion, while to a maximum of (0 deg, or 0 rad), at knee extension.

No Disturbance case

To assess the controller's performance, it must be ran without any payload (no human torque impact $\tau_h = 0$) and without any disruptions or noises. FADRC1, FADRC2 and FADRC3 performances are shown in Figure 4. (Desired vs Real output). Figure 5 depicts the difference in the knee position between the desired and actual positions for all controllers. The FADRC3 control approach achieves the least tracking error, proving its effectiveness and superiority to FRADC1 and FADRC2, as shown in Table 2, with the smallest R.M.S.E (0.0039). When comparing the performance index (R.M.S.E) for the best case of FADRC2 and the proposed FADRC3, a reduction of 48 % is observed. It can be stated that the FADRC3 controller outperforms the FADRC1 and FADRC2 controllers due to the additional degree of freedom.

Figure 6 depicts the control efforts required to study the control torque (τ_c) or $u(t)$ for all control systems. When compared to FADRC1 and FADRC2, the experimental results reveal that the FADRC3 control approach produces the smallest control effort required for a controller (ISU = 108) and the largest measure of chattering reduction in the control signal index (IAU = 39.63) due to the presence of two fractional terms, one at the feedback path (FESO) and the other at the feedforward path (FPD), as can be seen in Table 3.

With Disturbance case

In this case, the performance of the proposed controller under disturbance application is assessed. The joint position is measured practically by an absolute encoder mounted at the rotational shaft of knee joint, which may cause a noise in the measurement. A noise can also be produced by the exoskeleton user during the training. It considers a condition of disturbance by a payload of 0.5 kg, which is introduced in between the flexion/extension at 2 s cycle as shown in Figure 7.

Figure 8 shows the position trajectory performance and how the FADRC3 compensates this effect and returns the trajectory to the desired path in a period of less than 0.2 s. Figure 9 shows the trajectory error, where the FADRC3 approach, at a steady-state condition, has the smallest error (R.M.S.E = 0.0091) when compared to FADRC1 and FADRC2, as shown in Table 4. Figure 10 depicts the control efforts required to study the control torque (τ_c) or $u(t)$ for all control systems. When compared to FADRC1 and FADRC2, the experimental results reveal that the FADRC3 control approach produces the smallest control effort required for a controller (ISU = 115.74) and the largest measure of chatter reduction in the control signal index (IAU = 46.82). Table 5 shows the comparative experiment results. Since FADRC3 is the better approach for a more accurate tracking when compared with other approaches, we can focus on the effectives of ESO (which is the key aspect of ADRC), Figure 11 shows how the estimate $x_3(t)$ follows its total disturbance target $(\hat{\delta})$. It is clearly shown that estimate $x_3(t)$ tracks total disturbances very closely, especially at a steady-state condition. As seen from Table 4 and Table 5, all indices are increased with disturbance, which is the desired behaviour due to the disturbance effect.

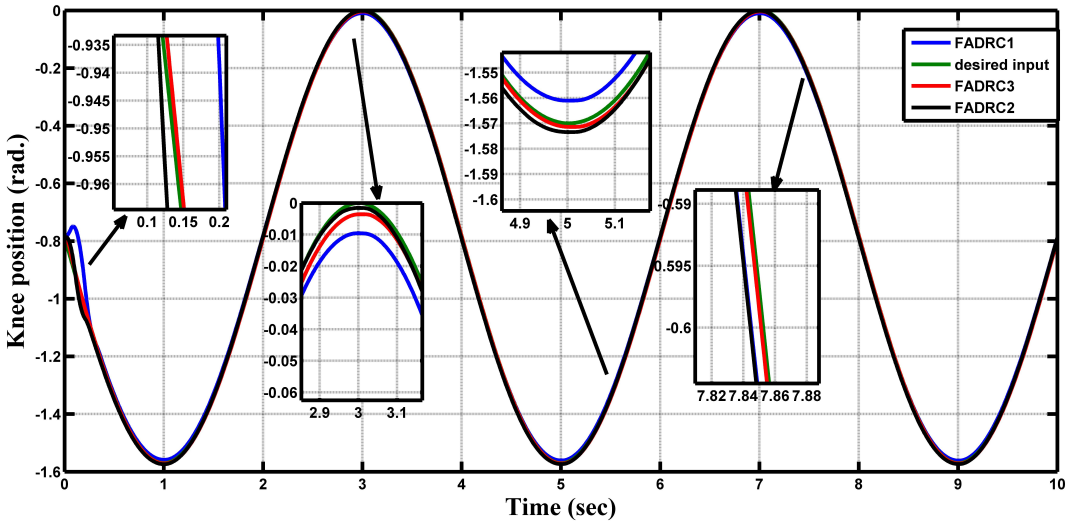

FIGURE 4. Knee position trajectory for comparison of all controllers.

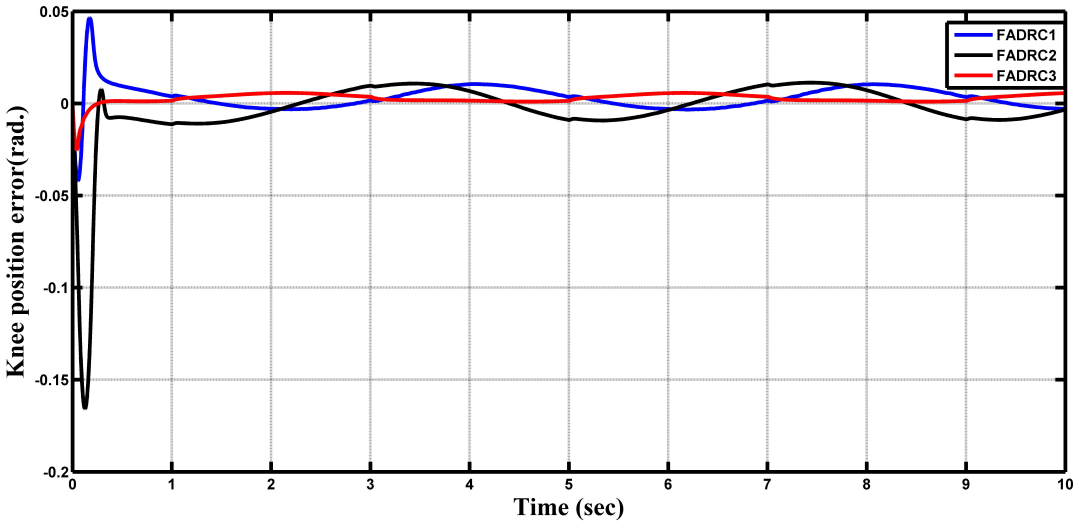

FIGURE 5. Knee position error for comparison of all controllers.

Control methods	IAE [rad]	ISE [rad]	R.M.S.E [rad]
FADRC1	0.028	0.000129	0.0184
FADRC2	0.023	0.000116	0.0075
FADRC3	0.012	0.000101	0.0039
Reduction [%]	47.8	13	48

TABLE 2. Performance error indices for all controllers without disturbance.

Control methods	ISU [N·m]	ISE [N·m]
FADRC1	145.62	34.76
FADRC2	120	27.22
FADRC3	108	39.63

TABLE 3. Performance control signal indices for all controllers without disturbance.

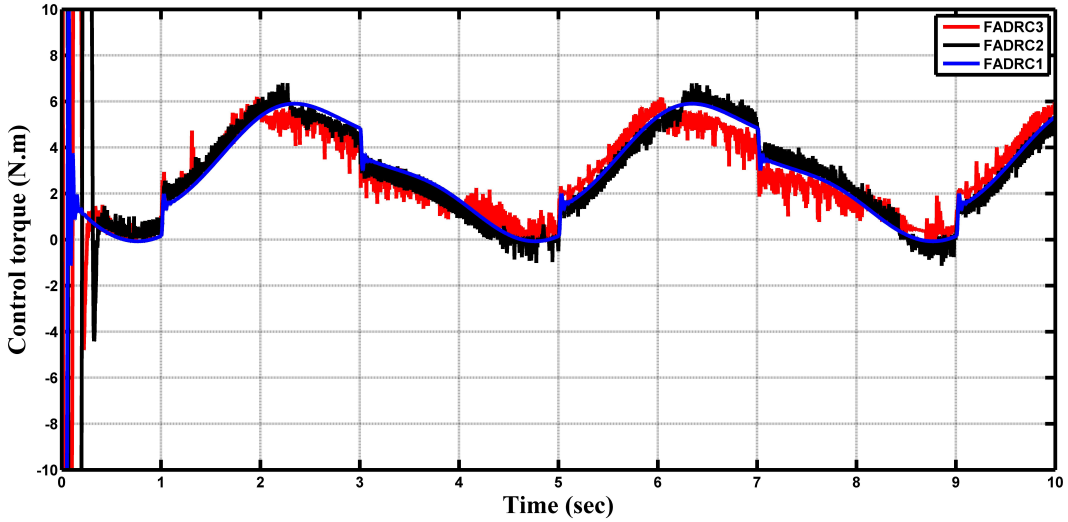

FIGURE 6. Control torque required comparison of all controllers.

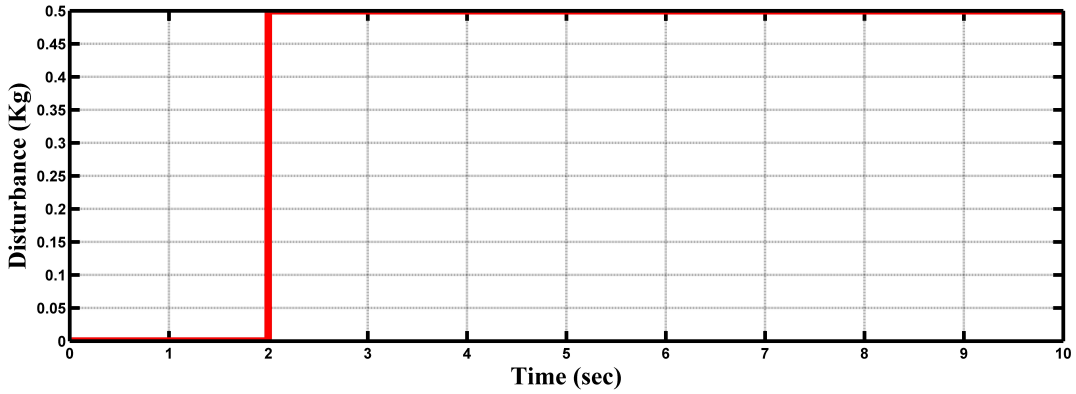

FIGURE 7. Constant disturbance payload.

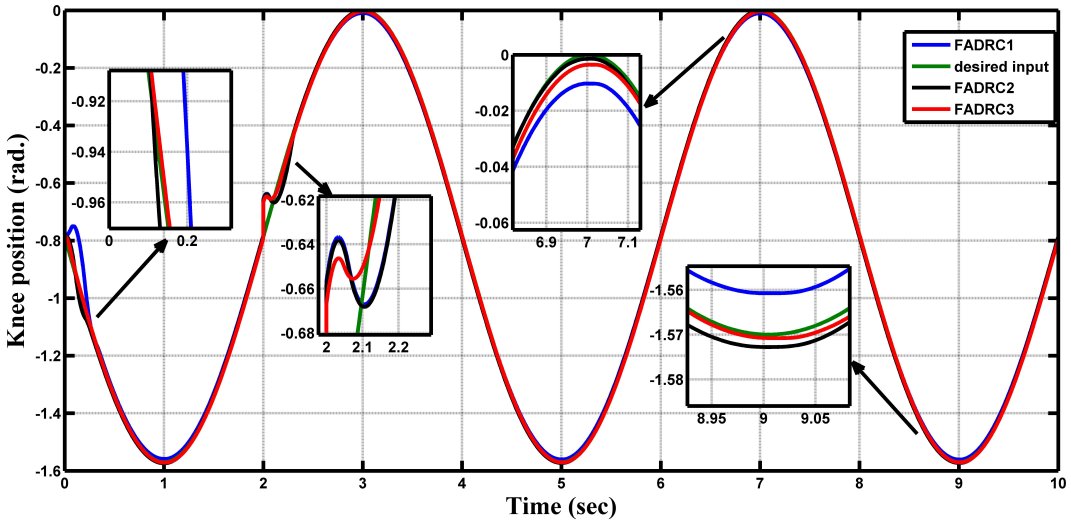

FIGURE 8. Knee position trajectory for comparison of all controllers with disturbance.

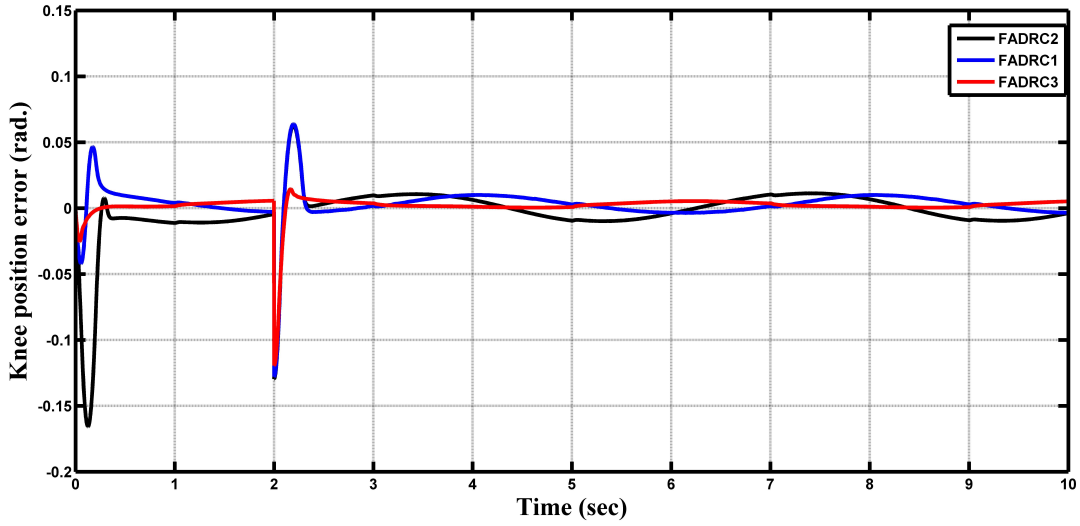

Figure 9. Knee position error for comparison of all controllers with disturbance.

Control methods	IAE [rad]	ISE [rad]	R.M.S.E [rad]
FADRC1	0.112	0.004943	0.0225
FADRC2	0.066	0.000891	0.0137
FADRC3	0.035	0.000796	0.0091
Reduction [%]	46.37	11	33.5

Table 4. Performance error indices for all controllers with disturbance.

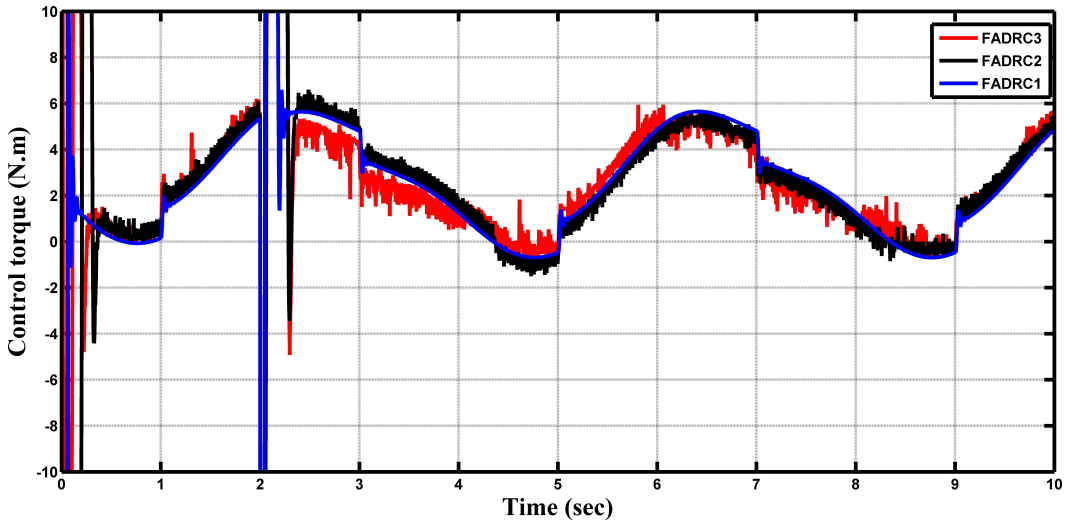

Figure 10. Control torque required comparison of all controllers with disturbance.

Control methods	ISU [N·m]	ISE [N·m]
FADRC1	157.83	38.93
FADRC2	127.58	25.32
FADRC3	115.74	46.82

Table 5. Performance control signal indices for all controllers with disturbance.

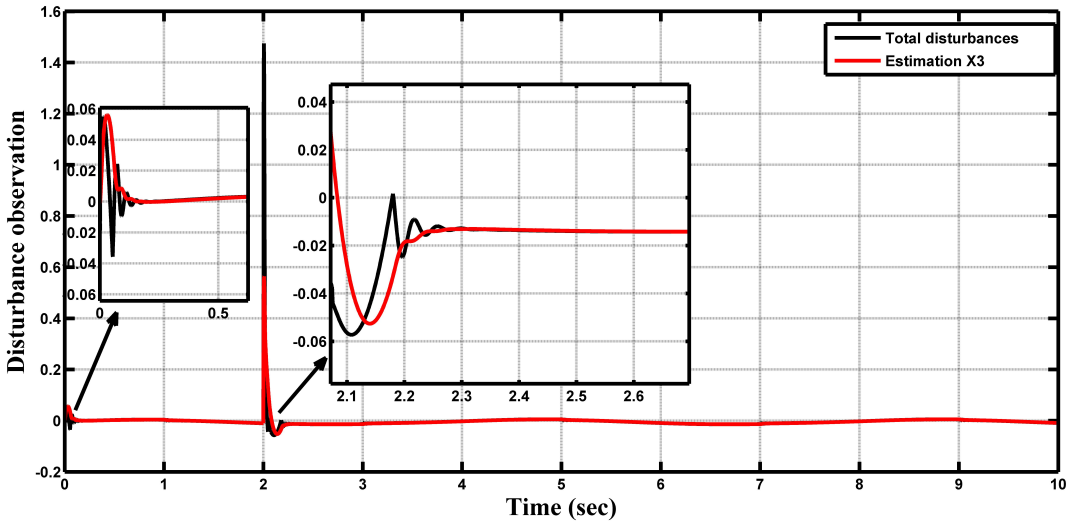

FIGURE 11. Total disturbances and its estimation of FADRC3 with disturbance.

5. CONCLUSIONS

An FADRC controller has been devised in this research to reduce the lower exoskeleton tracking error for a knee joint motion. To compensate for the effects of unstructured disturbances, the ADRC controller includes a fractional term in both paths, feedback and feedforward (FADRC3). There is a comparison of the tracking responses of the proposed FADRC3 and FADRC controllers, one with the fractional term in the feedforward path (FADRC1) and the second one with the fractional term the in feedback path (FADRC2). The suggested control methods are implemented in the Exoskeleton Intelligently Communicating and Sensitive to Intention (EICoSI) model of a knee exoskeleton. As a result, many findings were reached. This technique combines the advantages of the fractional order robustness with the efficiency of the ADRC controller. A single-leg flexible exoskeleton was used to test this technology. The dynamic model was reorganised to become an extended state space. A fractional order ADRC was utilised to actively estimate this disturbance via ESO, with a FPD feedback controller subsequently compensating it. The suggested controller outperforms the typical ADRC controller due to the extra degree of freedom in the Fractional (PD and ESO). The simulation results demonstrate that the tracking errors obtained with the suggested FADRC3 are lower than those obtained with the typical FADRC1 and FADRC2 controllers. The usefulness of the suggested controller was demonstrated by a numerical simulation and several performances indices. It can actively estimate the impact of an external disturbance during each sampling period and then compensate for it. Finally, FADRC3 is an excellent Exoskeleton system control strategy when compared with FADRC1 and FADRC2, as can be seen from numerical results according to performance indices for the tracking error (R.M.S.E) and control signal required (ISU), with a minimal chattering due to the fractional terms in ESO and PD controller. Numerically, the R.M.S.E of FADRC3 without disturbance is (0.0039 rad), and (0.0091 rad) with disturbance. These values are the smallest when compared with other controllers, the same can be said for the control efforts (ISU).

This study can be continued by implementing the suggested control method in a real-time context with FPGA [56]. Utilising modern optimisation techniques to adjust the design parameters for the suggested controller's optimum performance is another continuation of this work [57, 58]. Additionally, the performance of the suggested controller can be compared to alternative control methods [59–64].

REFERENCES

[1] A. M. Dollar, H. Herr. Lower extremity exoskeletons and active orthoses: Challenges and state-of-the-art. *IEEE Transactions on Robotics* **24**(1):144–158, 2008. https://doi.org/10.1109/TRO.2008.915453

[2] R. Baud, A. R. Manzoori, A. Ijspeert, M. Bouri. Review of control strategies for lower-limb exoskeletons to assist gait. *Journal of NeuroEngineering Rehabilitation* **18**:119, 2031. https://doi.org/10.1186/s12984-021-00906-3

[3] C. Carignan, J. Tang, S. Roderick. Development of an exoskeleton haptic interface for virtual task training. In *2009 IEEE/RSJ International Conference on Intelligent Robots and Systems*, pp. 3697–3702. 2009. https://doi.org/10.1109/IROS.2009.5354834

[4] H. Zhang, S. Balasubramanian, R. Wei, et al. RUPERT closed loop control design. In *2010 Annual International Conference of the IEEE Engineering in Medicine and Biology*, pp. 3686–3689. 2010. https://doi.org/10.1109/IEMBS.2010.5627647

[5] K. Suzuki, Y. Kawamura, T. Hayashi, et al. Intention-based walking support for paraplegia patient. In *2005 IEEE International Conference on Systems,*

Man and Cybernetics, vol. 3, pp. 2707–2713. 2005. https://doi.org/10.1109/ICSMC.2005.1571559

[6] H. Kazerooni, J.-L. Racine, L. Huang, R. Steger. On the control of the Berkeley Lower Extremity Exoskeleton (BLEEX). In *Proceedings of the 2005 IEEE International Conference on Robotics and Automation*, pp. 4353–4360. 2005. https://doi.org/10.1109/ROBOT.2005.1570790

[7] H. K. Khalil. *Nonlinear Systems*. Pearson Education. Prentice Hall, 2002.

[8] M. Khamar, M. Edrisi. Designing a backstepping sliding mode controller for an assistant human knee exoskeleton based on nonlinear disturbance observer. *Mechatronics* **54**:121–132, 2018. https://doi.org/10.1016/j.mechatronics.2018.07.010

[9] M.-K. Chang. An adaptive self-organizing fuzzy sliding mode controller for a 2-DOF rehabilitation robot actuated by pneumatic muscle actuators. *Control Engineering Practice* **18**(1):13–22, 2010. https://doi.org/10.1016/j.conengprac.2009.08.005

[10] S. M. Taslim Reza, N. Ahmad, I. A. Choudhury, R. A. R. Ghazilla. A fuzzy controller for lower limb exoskeletons during sit-to-stand and stand-to-sit movement using wearable sensors. *Sensors* **14**(3):4342–4363, 2014. https://doi.org/10.3390/s140304342

[11] T. H. Do, D. T. Vu. An intelligent control for lower limb exoskeleton for rehabilitation. *SSRG International Journal of Electrical and Electronics Engineering* **4**(8):13–19, 2017. https://doi.org/10.14445/23488379/IJEEE-V4I8P103

[12] L. Vaca Benitez, M. Tabie, N. Will, et al. Exoskeleton technology in rehabilitation: Towards an emg-based orthosis system for upper limb neuromotor rehabilitation. *Journal of Robotics* **2013**:610589, 2013. https://doi.org/10.1155/2013/610589

[13] C. Caulcrick, W. Huo, E. Franco, et al. Model predictive control for human-centred lower limb robotic assistance. *IEEE Transactions on Medical Robotics and Bionics* **3**(4):980–991, 2021. https://doi.org/10.1109/TMRB.2021.3105141

[14] D. Sun. Comments on active disturbance rejection control. *IEEE Transactions on Industrial Electronics* **54**(6):3428–3429, 2007. https://doi.org/10.1109/TIE.2007.909047

[15] W. R. Abdul-Adheem, A. T. Azar, I. K. Ibraheem, A. J. Humaidi. Novel active disturbance rejection control based on nested linear extended state observers. *Applied Sciences* **10**(12):4069, 2020. https://doi.org/10.3390/app10124069

[16] R. Pérez-San Lázaro, I. Salgado, I. Chairez. Adaptive sliding-mode controller of a lower limb mobile exoskeleton for active rehabilitation. *ISA Transactions* **109**:218–228, 2021. https://doi.org/10.1016/j.isatra.2020.10.008

[17] M. Babaiasl, S. N. Goldar, M. H. Barhaghtalab, V. Meigoli. Sliding mode control of an exoskeleton robot for use in upper-limb rehabilitation. In *2015 3rd RSI International Conference on Robotics and Mechatronics (ICROM)*, pp. 694–701. 2015. https://doi.org/10.1109/ICRoM.2015.7367867

[18] B. S. K. K. Ibrahim, R. Ngadengon, M. N. Ahmad. Genetic algorithm optimized integral sliding mode control of a direct drive robot arm. In *2012 International Conference on Control, Automation and Information Sciences (ICCAIS)*, pp. 328–333. 2012. https://doi.org/10.1109/ICCAIS.2012.6466612

[19] A. Humaidi, M. Hameed. Development of a new adaptive backstepping control design for a non-strict and under-actuated system based on a PSO tuner. *Information* **10**(2):38, 2019. https://doi.org/10.3390/info10020038

[20] A. Al-qassar, A. Abdulkareem, A. Hasan, et al. Grey-Wolf optimization better enhances the dynamic performance of roll motion for tail-sitter VTOL aircraft guided and controlled by STSMC. *Journal of Engineering Science and Technology* **16**:1932–1950, 2021.

[21] L. Rasheed. Optimal tuning of linear quadratic regulator controller using ant colony optimization algorithm for position control of a permanent magnet DC motor. *Iraqui Journal of Computers, Cmmunications, Control and Systems Engineering* **20**(3):29–41, 2020. https://doi.org/10.33103/uot.ijccce.20.3.3

[22] S. Got, M. Lee, M. Park. Fuzzy-sliding mode control of a polishing robot based on genetic algorithm. *KSME International Journal* **15**:580–591, 2001. https://doi.org/10.1007/BF03184374

[23] S. M. Mahdi, N. Q. Yousif, A. A. Oglah, et al. Adaptive synergetic motion control for wearable knee-assistive system: A rehabilitation of disabled patients. *Actuators* **11**(7):176, 2022. https://doi.org/10.3390/act11070176

[24] A. J. Humaidi, A. A. Mohammed, A. H. Hameed, et al. State estimation of rotary inverted pendulum: A comparative study of observers performance. In *2020 IEEE Congreso Bienal de Argentina (ARGENCON)*, pp. 1–7. 2020. https://doi.org/10.1109/ARGENCON49523.2020.9505507

[25] J. Han. From PID to active disturbance rejection control. *IEEE Transactions on Industrial Electronics* **56**(3):900–906, 2009. https://doi.org/10.1109/TIE.2008.2011621

[26] H. Yang, Y. Yu, J. Zhang. Angle tracking of a pneumatic muscle actuator mechanism under varying load conditions. *Control Engineering Practice* **61**:1–10, 2017. https://doi.org/10.1016/j.conengprac.2017.01.008

[27] Y. Long, Z. Du, L. Cong, et al. Active disturbance rejection control based human gait tracking for lower extremity rehabilitation exoskeleton. *ISA Transactions* **67**:389–397, 2017. https://doi.org/10.1016/j.isatra.2017.01.006

[28] Y. Chen, Y. Wei, X. Zhou, et al. Stability for nonlinear fractional order systems: An indirect approach. *Nonlinear Dynamics* **89**:1011–1018, 2017. https://doi.org/10.1007/s11071-017-3497-y

[29] A. Jmal, O. Naifar, A. Ben Makhlouf, et al. Adaptive stabilization for a class of fractional-order systems with nonlinear uncertainty. *Arabian Journal for Science and Engineering* **45**:2195–2203, 2020. https://doi.org/10.1007/s13369-019-04148-3

[30] A. Abid, R. Jallouli-Khlif, N. Derbel, P. Melchior. *Crone Controller Design for a Robot Arm*, pp. 187–200. Springer Singapore, Singapore, 2019. https://doi.org/10.1007/978-981-13-2212-9_8

[31] H. Delavari, R. Ghaderi, N. Ranjbar, et al. Adaptive fractional PID controller for robot manipulator. In *The 4th IFAC Workshop Fractional Differentiation and its Applications*, vol. FDA10-038, pp. 18–20. 2010. https://doi.org/10.48550/arXiv.1206.2027

[32] S. Ahmed, H. Wang, Y. Tian. Robust adaptive fractional-order terminal sliding mode control for lower-limb exoskeleton. *Asian Journal of Control* **21**(1):473–482, 2019. https://doi.org/10.1002/asjc.1964

[33] P. Shah, S. Agashe. Review of fractional PID controller. *Mechatronics* **38**:29–41, 2016. https://doi.org/10.1016/j.mechatronics.2016.06.005

[34] I. Zaway, R. Jallouli-Khlif, B. Maalej, et al. From PD to fractional order PD controller used for gait rehabilitation. In *2021 18th International Multi-Conference on Systems, Signals and Devices (SSD)*, pp. 948–953. 2021. https://doi.org/10.1109/SSD52085.2021.9429318

[35] D. Li, P. Ding, Z. Gao. Fractional active disturbance rejection control. *ISA Transactions* **62**:109–119, 2016. https://doi.org/10.1016/j.isatra.2016.01.022

[36] J. Song, J. Lin, L. Wang, et al. Nonlinear FOPID and active disturbance rejection hypersonic vehicle control based on DEM biogeography-based optimization. *Journal of Aerospace Engineering* **30**(6):04017079, 2017. https://doi.org/10.1061/(ASCE)AS.1943-5525.0000786

[37] B. Pradhan, X. Zhou, C. Yang, et al. A high-precision control scheme based on active disturbance rejection control for a three-axis inertially stabilized platform for aerial remote sensing applications. *Journal of Sensors* **2018**:7295852, 2018. https://doi.org/10.1155/2018/7295852

[38] R. S. Al-Azzawi, M. A. Simaan. On the selection of leader in Stackelberg games with parameter uncertainty. *International Journal of Systems Science* **52**(1):86–94, 2021. https://doi.org/10.1080/00207721.2020.1820097

[39] P. Chen, Y. Luo, W. Zheng, Z. Gao. A new active disturbance rejection controller design based on fractional extended state observer. In *2019 Chinese Control Conference (CCC)*, pp. 4276–4281. 2019. https://doi.org/10.23919/ChiCC.2019.8865339

[40] F. Hongqing, Y. Xinjian, L. Peng. Active-disturbance-rejection-control and fractional-order-proportional-integral-derivative hybrid control for hydroturbine speed governor system. *Measurement and Control* **51**(5-6):192–201, 2018. https://doi.org/10.1177/0020294018778312

[41] S. Mefoued, D. Belkhiat. A robust control scheme based on sliding mode observer to drive a knee-exoskeleton. *Asian Journal of Control* **21**(1):439–455, 2019. https://doi.org/10.1002/asjc.1950

[42] R. Mallat, V. Bonnet, G. Venture, et al. Dynamics assessment and minimal model of an orthosis-assisted knee motion. In *2020 8th IEEE RAS/EMBS International Conference for Biomedical Robotics and Biomechatronics (BioRob)*, pp. 352–357. 2020. https://doi.org/10.1109/BioRob49111.2020.9224432

[43] P. A. Mozuca, J. D. Gallo, R. I. Rincon, G. A. Ramos. Performance of different ADRC based control methods in a nonlinear plant with uncertainties. In *2019 IEEE 4th Colombian Conference on Automatic Control (CCAC)*, pp. 1–6. 2019. https://doi.org/10.1109/CCAC.2019.8921151

[44] W. R. Abdul-Adheem, I. K. Ibraheem, A. J. Humaidi. Model-free active input–output feedback linearization of a single-link flexible joint manipulator: An improved active disturbance rejection control approach. *Measurement and Control* **54**(5-6):856–871, 2011. https://doi.org/10.1177/0020294020917171

[45] X. Chen, D. Li, Z. Gao, C. Wang. Tuning method for second-order active disturbance rejection control. In *Proceedings of the 30th Chinese Control Conference*, pp. 6322–6327. 2011.

[46] R. Caponetto, E. C. de Oliveira, J. A. Tenreiro Machado. A review of definitions for fractional derivatives and integral. *Mathematical Problems in Engineering* **2014**:238459, 2014. https://doi.org/10.1155/2014/238459

[47] N. Alawad, A. Humaidi, A. Alaraji. Fractional proportional derivative-based active disturbance rejection control of knee exoskeleton device for rehabilitation care. *Indonesian Journal of Electrical Engineering and Computer Science* **28**(3):1405–1413, 2014. https://doi.org/10.11591/ijeecs.v28.i3.pp1405-1413

[48] M. Zamani, M. Karimi-Ghartemani, N. Sadati, M. Parniani. Design of a fractional order PID controller for an AVR using particle swarm optimization. *Control Engineering Practice* **17**(12):1380–1387, 2009. https://doi.org/10.1016/j.conengprac.2009.07.005

[49] A. Humaidi, H. Badr. Linear and nonlinear active disturbance rejection controllers for single-link flexible joint robot manipulator based on PSO tuner. *Journal of Engineering Science and Technology Review* **11**(3):133–138, 2018. https://doi.org/10.25103/jestr.113.18

[50] J.-Y. Cao, J. Liang, B.-G. Cao. Optimization of fractional order PID controllers based on genetic algorithms. In *2005 International Conference on Machine Learning and Cybernetics*, vol. 9, pp. 5686–5689. 2005. https://doi.org/10.1109/ICMLC.2005.1527950

[51] M. Y. Hassan, A. J. Humaidi, M. K. Hamza. On the design of backstepping controller for acrobot system based on adaptive observer. *International Review of Electrical Engineering* **15**(4):328–335, 2020. https://doi.org/10.15866/iree.v15i4.17827

[52] N. Alawad, A. Humaidi, A. Al-Araji. Improved active disturbance rejection control for the knee joint motion model. *Mathematical Modelling of Engineering Problems* **9**(2):477–483, 2022. https://doi.org/10.18280/mmep.090225

[53] I. Ibraheem, W. Abdul-Adheem. On the improved nonlinear tracking differentiator based nonlinear PID controller design. *International Journal of Advanced Computer Science and Applications* **7**(10):234–241, 2016. https://doi.org/10.14569/IJACSA.2016.071032

[54] Y. Aydin, O. Tokatli, V. Patoglu, C. Basdogan. Stable physical human-robot interaction using fractional order admittance control. *IEEE Transactions on Haptics* **11**(3):464–475, 2018. https://doi.org/10.1109/TOH.2018.2810871

[55] P. Chen, Y. Luo, W. Zheng, et al. Fractional order active disturbance rejection control with the idea of cascaded fractional order integrator equivalence. *ISA Transactions* **114**:359–369, 2021. https://doi.org/10.1016/j.isatra.2020.12.030

[56] M. Q. Kasim, R. F. Hassan, A. J. Humaidi, et al. Control algorithm of five-level asymmetric stacked converter based on Xilinx system generator. In *2021 IEEE 9th Conference on Systems, Process and Control (ICSPC 2021)*, pp. 174–179. 2021. https://doi.org/10.1109/ICSPC53359.2021.9689173

[57] A. J. Humaidi, S. K. Kadhim, A. S. Gataa. Optimal adaptive magnetic suspension control of rotary impeller for artificial heart pump. *Cybernetics and Systems* **53**(1):141–167, 2022. https://doi.org/10.1080/01969722.2021.2008686

[58] O. Wanhab, A. Al-Araji. An optimal path planning algorithms for a mobile robot. *Iraqi Journal of Computers, Communications, Control and Systems Engineering* **21**(2):44–58, 2021. https://doi.org/10.33103/uot.ijccce.21.2.4

[59] F. Hussein, S. Raafat. Optimal linear quadratic control for knee-ankle orthosis system. *Iraqi Journal of Computers, Communications, Control and Systems Engineering* **22**(2):109–124, 2022. https://doi.org/10.33103/uot.ijccce.22.2.10

[60] N. Alawad, A. Humaidi, A. Alaraji. Observer sliding mode control design for lower exoskeleton system: Rehabilitation case. *Journal of Robotics and Control* **3**(4):476–482, 2022. https://doi.org/10.18196/jrc.v3i4.15239

[61] N. Ahmed, A. Humaidi, A. Sabah. Clinical trajectory control for lower knee rehabilitation using ADRC method. *Journal of Applied Research and Technology* **20**(5):576–583, 2022. https://doi.org/10.22201/icat.24486736e.2022.20.5.1920

[62] N. Alawad, A. Humaidi, A. Al-Obaidi, A. Alaraj. Active disturbance rejection control of wearable lower limb system based on reduced ESO. *Indonesian Journal of Science and Technology* **7**(2):203–218, 2022. https://doi.org/10.17509/ijost.v7i2.46435

[63] S. Husain, M. Kadhim, A. Al-Obaidi, et al. Design of robust control for vehicle steer-by-wire system. *Indonesian Journal of Science and Technology* **8**(2):197–216, 2023. https://doi.org/10.17509/ijost.v8i2.54794

[64] N. A. Al-Awad. Model reference adaptive control-based genetic algorithm desing for heading ship motion. *Acta Polytechnica* **60**(3):197–205, 2020. https://doi.org/10.14311/AP.2020.60.0197